

# A density- and stress-dependent elasto-plastic model for sands subjected to monotonic undrained torsional shear loading

G. Chiaro<sup>1</sup>, J. Koseki<sup>2</sup> and L.I. Nalin De Silva<sup>3</sup>

<sup>1</sup>Centre for Geomechanics and Railway Engineering, University of Wollongong, Wollongong, Australia

<sup>2</sup>Institute of Industrial Science, University of Tokyo, Tokyo, Japan

<sup>3</sup>Department of Civil Engineering, University of Moratuwa, Sri Lanka

E-mails: gchiaro@uow.edu.au; koseki@iis.u-tokyo.ac.jp; nalinds@uom.lk

**ABSTRACT:** A density- and stress-dependent elasto-plastic model for saturated sands undergoing monotonic undrained torsional shear loading is presented in this paper. The model is developed under an extended general hyperbolic equation (GHE) approach, in which the void ratio and stress level dependence upon stress-strain response of sand is incorporated. Most importantly, a state-dependent stress-dilatancy relationship is introduced to account for the effect of density on the stress ratio. Such a stress-dilatancy relation is used for modeling the excess pore water pressure generation in undrained shear conditions as the mirror effect of volumetric change in drained shear conditions. In this paper, details of the model formulation and soil parameters calibration are described. By using the proposed model, numerical simulation of monotonic undrained torsional shear tests have been carried out on Toyoura sand. The model predictions show that undrained shear behavior, described in terms of stress-strain relationship and effective stress path for both loose and dense sands can be modeled satisfactorily by using a single set of soil parameters.

## 1. INTRODUCTION

Sand behaves differently under different density states and confining pressures as well as loading conditions (e.g. triaxial compression and extension, plane strain, simple shear, torsional shear etc) as widely reported in the literature (e.g. Tatsuoka *et al.*, 1982; Ishihara, 1993; Verdugo and Ishihara, 1996; Yoshimine and Ishihara, 1998; Nishimura and Towhata, 2004; Georgiannou *et al.*, 2008). In view of its complex behavior, to predict in a very straightforward and reliable manner the response of sand undergoing monotonic shear loadings for a large range of initial void ratios and confining pressures without the need to make any change to the soil parameters remains a major challenge in geomechanics. Although in the last few decades, several constitutive models have been proposed, each of them was with varying extent of capability and applicability.

In models based on generalized plasticity (e.g. Pastor *et al.*, 1990; Ling and Liu, 2003), complex mathematical formulations are often used. In addition, the same sand is usually considered as different material depending on its density and stress level, so that a large number of soil parameters is required. Alternatively, one advantage of critical-state constitutive models (e.g. Jefferies, 1993; Imam *et al.*, 2005; Modoni *et al.*, 2011) is their ability to predict soil behavior over a range of densities and confining pressures by using a single set of soil parameters. In the work done by Ling and Yang (2006), a unified model based on critical state and generalized plasticity has been proposed. Nevertheless, there may be debates over the uniqueness of the critical state line (e.g. Vaid *et al.*, 1990; Yamamuro and Lade, 1998; Modoni and Gazzellone, 2011; Li and Dafalias, 2012). In addition, the majority of such predictive models has been validated only for the case of triaxial loadings.

It is widely recognized that hyperbolic equations can be used to model the highly non-linear stress-strain behavior of soil subjected to shear loading (Kondner, 1963; Duncan and Chang, 1970; Hardin and Drnevich, 1972; Tatsuoka and Shibuya, 1992; Cubrinovski and Ishihara, 1998a,b). In particular, the general hyperbolic equation (GHE) proposed by Tatsuoka and Shibuya (1992) can properly simulate stress-strain relations from very small to large strain levels for a wide range of geomaterials under general loading conditions (Tatsuoka *et al.*, 1993; Balakrishnan, 2000; Tatsuoka *et al.*, 2003; HongNam, 2004; HongNam and Koseki, 2005; De Silva, 2008; Chiaro, 2010; Chiaro *et al.*, 2011; De Silva *et al.*, 2012).

De Silva (2008) successfully used a GHE combined with an empirical stress-dilatancy equation to simulate the overall behavior of Toyoura sand undergoing drained/undrained monotonic/cyclic torsional shear loading conditions. Later, Chiaro (2010) incorporated into this model the effect of initial static shear stress.

However, neither the density nor the combined influence of density and stress level was considered as a variable. To be precise, sand with different densities was regarded as different material and the effects of confining pressure were considered to be independent from the density state. As a consequence, a number of soil parameters were needed for simulating different density and stress level conditions.

In this paper, following the achievement of De Silva (2008) and Chiaro (2010), an elasto-plastic model that deals with density and stress level dependency upon undrained behavior of sand, using the GHE approach combined with an empirical stress-dilatancy equation, is presented. The proposed model is able to predict sand behavior in monotonic undrained torsional shear tests over a wide range of void ratios and confining pressures using a single set of soil parameters.

From a practical viewpoint, some advantages of the proposed model are its mathematical simplicity and the use of a single set of soil parameters. If implemented in an FEM code, it would represent a useful tool for researchers and practicing engineers to study complex liquefaction soil problems where density and stress level are likely to change significantly from place to place within a sand deposit.

## 2. MONOTONIC UNDRAINED BEHAVIOR OF SAND

When sand is subjected to shear load, it exhibits very complex behavior, which is governed by the initial state of density and stress level. Typical behavior of sand specimens isotropically consolidated at different density levels and subjected to monotonic undrained shear loading is described in Figures 1(a) and 1(b), in terms of effective stress path and stress-strain relationship, respectively.

*Very loose sand (path A-B-C).* Very loose sand generally exhibits a purely contractive behavior, during which effective mean stress ( $p'$ ) decreases while shear stress ( $\tau$ ) progressively increases up to a transient peak stress (point B). The peak stress state is accompanied by an unstable behavior (Lade, 1993) with a sudden loss of strength and a large development of pore water pressure and shear strains. Finally, at point C, soil deforms under a nearly constant stress (i.e. steady state; Verdugo and Ishihara, 1996). In addition, by looking at the stress-strain response, strain-softening behavior (i.e. decrease in shear strength owing to shear strain increase) can be observed after the transient peak stress. Due to its fully contractive response, loose sand is expected to experience full liquefaction state ( $p' = 0$ ) with zero residual shear strength ( $\tau = 0$ ).

*Loose/medium dense sand (path A-D-E-F).* Alternatively, loose sand shows a contractive behavior until the stress state reaches the phase transformation (Ishihara *et al.*, 1975) at point E. Then dilative

behavior takes place and the effective stress path increases while following the failure envelope line (path E-F).

**Dense sand (path A-G-H).** Dense sand presents a significantly different behavior. Contractive behavior is markedly reduced so that the unstable behavior is no longer observed (i.e. no transient peak stress). Dilative behavior begins when stress state achieves the phase transformation (point G), usually at a higher value of  $p'$  as compared with loose sands, and then the effective stress path follows the failure envelope line (path G-H). Moreover, strain-hardening behavior (i.e. increase in shear stress caused by shear strain increase) can be observed by looking at the stress-strain relationship.

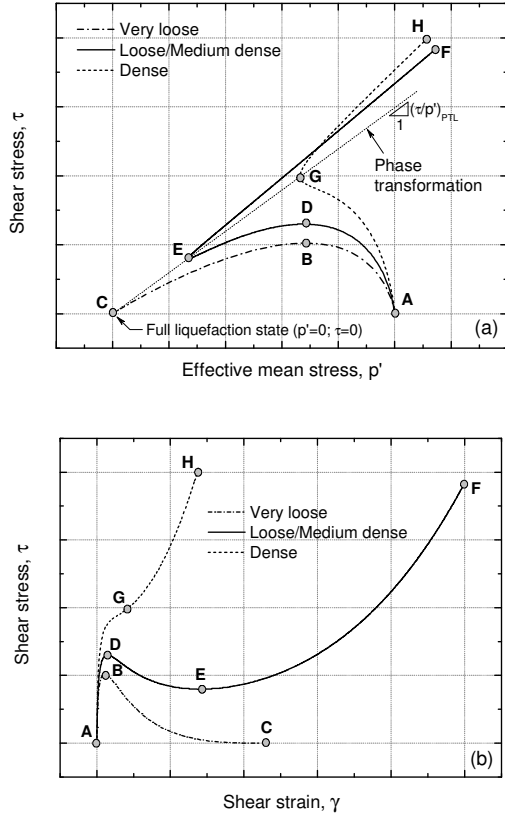


Figure 1 Pattern of monotonic undrained torsional shear behavior of sand consolidated at different densities

### 3. STRESSES AND STRAINS IN TORSIONAL SHEAR

During earthquakes, idealised field stress conditions are like those in simple shear and can be reproduced by using a hollow cylinder torsional shear apparatus (e.g. Tatsuoka *et al.*, 1982; Georgiannou *et al.*, 2008; Kiyota *et al.*, 2008; Chiaro *et al.* 2012 and 2013).

Four independently loading components, namely vertical axial load ( $F_z$ ), torque load ( $T$ ), inner cell pressure ( $p_i$ ) and outer cell pressure ( $p_o$ ) can be applied (Figure 2) and the correspondent four stress components i.e. axial stress ( $\sigma_z$ ), radial stress ( $\sigma_r$ ), circumferential stress ( $\sigma_\theta$ ) and torsional shear stress ( $\tau_{z\theta}$ ) can be generated. The relation between the above stress (i.e. in terms of average stress) and loading components can be defined as follows (Hight *et al.*, 1983):

$$\sigma_z = \frac{F_z}{\pi(r_o^2 - r_i^2)} + \frac{(p_o r_o^2 - p_i r_i^2)}{(r_o^2 - r_i^2)} \quad (1)$$

$$\sigma_r = \frac{(p_o r_o + p_i r_i)}{(r_o + r_i)} \quad (2)$$

$$\sigma_\theta = \frac{(p_o r_o - p_i r_i)}{(r_o - r_i)} \quad (3)$$

$$\tau = \tau_{z\theta} = \frac{3T}{2\pi(r_o^3 - r_i^3)} \quad (4)$$

where  $r_o$  and  $r_i$  are the outer and inner radius of the specimen, respectively;  $\theta$  is the circumferential angular displacement and  $H$  is the specimen height.

The average main stresses  $\sigma_1$  (major),  $\sigma_2$  (intermediate),  $\sigma_3$  (minor) as well as the mean stress  $p$  are given by:

$$\left\{ \begin{matrix} \sigma_1 \\ \sigma_3 \end{matrix} \right\} = \frac{\sigma_z + \sigma_\theta}{2} \pm \sqrt{\frac{(\sigma_z + \sigma_\theta)^2}{4} + \tau_{z\theta}^2} \quad (5)$$

$$\sigma_2 = \sigma_r \quad (6)$$

$$p = \frac{\sigma_1 + \sigma_2 + \sigma_3}{3} \quad (7)$$

In addition to averages stresses, the average torsional shear strain is defined as:

$$\gamma = \gamma_{z\theta} = \frac{2\theta}{3H} \frac{(r_o^3 - r_i^3)}{(r_o^2 - r_i^2)} \quad (8)$$

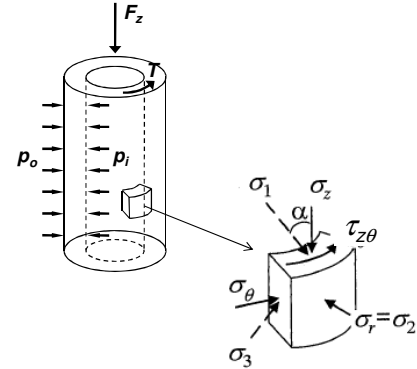


Figure 2 External forces and stress components acting on a hollow cylindrical specimen (Chiaro, 2010).

### 4. MODEL FORMULATIONS

The model is developed within a classical elasto-plastic framework, where shear strain increment ( $d\gamma$ ) is defined as the sum of elastic strain increment ( $d\gamma^e$ ) and plastic strain increment ( $d\gamma^p$ ):

$$d\gamma = d\gamma^e + d\gamma^p \quad (9)$$

Nevertheless, the model assumes that for any given shear stress increment ( $d\tau$ ) both elastic and plastic deformation do always occur, so that a purely elastic region does not exist i.e. sand continuously yields from the very small strains.

The plastic distortional and volumetric behavior of sand is specified by a pair of fundamental relations, namely GHE and stress-dilatancy relationship. Both relations include key parameters that are dependent on the amount of plastic shear strain as well as the initial state condition (i.e. void ratio and stress level). The contribution of elastic behavior is estimated using a quasi-elastic model proposed by HongNam and Koseki (2005), even though it might be smaller than that of plastic behavior.

#### 4.1 Plastic shear strain

The highly non-linear stress-strain behavior of sand subjected to shear loading can be modeled by using a GHE, which has been proposed by Tatsuoka and Shibuya (1992) in the form:

$$y = \frac{x}{\frac{1}{C_{1(x)}} + \frac{x}{C_{2(x)}}} \quad (10)$$

where  $x$  and  $y$  are two functions representing plastic shear strain and shear stress ratio, respectively.

Most importantly,  $C_{1(x)}$  and  $C_{2(x)}$  are two fitting parameters that vary with the strain level. They were introduced by Tatsuoka and Shibuya (1992) to simulate in a more realistic way such highly complicated non-linear stress-strain behavior of sand. For the case of torsional shear loading, they can be formulated as follows:

$$C_{1(x)} = \frac{C_{1(0)} + C_{1(\infty)}}{2} + \frac{C_{1(0)} - C_{1(\infty)}}{2} \cos\left\{\frac{\pi}{(\alpha/x)^a + 1}\right\} \quad (11)$$

$$C_{2(x)} = \frac{C_{2(0)} + C_{2(\infty)}}{2} + \frac{C_{2(0)} - C_{2(\infty)}}{2} \cos\left\{\frac{\pi}{(\beta/x)^b + 1}\right\} \quad (12)$$

All the coefficients ( $C_{1(0)}$ ,  $C_{1(\infty)}$ ,  $\alpha$ ,  $a$ ,  $C_{2(0)}$ ,  $C_{2(\infty)}$ ,  $\beta$ ,  $b$ ) in Eqns. (11) and (12) can be determined by fitting the experimental data plotted in terms of  $y/x$  vs.  $y$  relationship as detailed in Tatsuoka and Shibuya (1992). Note that  $C_{1(0)}$  is the initial normalized plastic shear modulus, while  $C_{2(\infty)}$  represents the normalized peak strength of the material.

De Silva (2008) and Chiaro (2010) demonstrated that if properly normalized, the stress-strain relationship of sand could be represented by a unique curve irrespective of density level and drainage conditions. In this current model, with the intention of incorporating into the GHE the void ratio and confining stress level dependence of stress-strain behavior of sand, the same  $x$  and  $y$  functions employed by De Silva (2008) and Chiaro (2010) were adopted:

$$y = \frac{\tau / p'}{(\tau / p')_{\max}} \quad (13)$$

$$x = \gamma^p / \gamma_{\text{ref}} \quad (14)$$

$$\gamma_{\text{ref}} = \frac{(\tau / p')_{\max}}{G_0 / p_0'} \quad (15)$$

where  $\gamma^p$  is the plastic shear strain;  $\tau$  is the shear stress;  $p'$  and  $p_0'$  are the current and initial effective mean stress, respectively;  $(\tau / p')_{\max}$  is the peak shear stress in the plot  $\tau / p'$  vs.  $\gamma^p$ ; and  $G_0$  is the initial shear modulus.

By substituting Eqns. (13), (14) and (15) into Eqn. (10) and using a few mathematical manipulations, the following expression is obtained:

$$\frac{\tau}{p'} = \frac{\gamma^p}{\frac{1}{(G_0 / p_0') C_{1(x)}} + \frac{\gamma^p}{(\tau / p')_{\max} C_{2(x)}}} \quad (16)$$

Note that in Eqn. (16), the dependence of void ratio ( $e_0$ ) and stress level ( $p_0'$ ) may be accounted by both  $G_0$  and  $(\tau / p')_{\max}$ , which are two parameters with clear physical meaning.

For clean sands, a number of empirical relationships have been proposed to relate  $G_0$  to the confining pressure and void ratio (e.g. Hardin and Richart, 1963; Iwasaki and Tatsuoka, 1977; Iwasaki et al., 1978). Above all, for the case of sand subjected to torsional shear loading, the following expression is valid:

$$G_0 = G_n f(e_0) (p_0' / p_{\text{ref}}')^n \quad (17)$$

$$f(e_0) = \frac{(2.17 - e_0)^2}{1 + e_0} \quad (18)$$

where  $G_n$  is a small strain shear stiffness parameter;  $p_{\text{ref}}'$  is a reference stress (=100 kPa) and  $n$  is a soil parameter to express the stress-level dependence of  $G_0$ . Both  $G_n$  and  $n$  are presented later for the case of Toyoura sand. Note that  $f(e_0)$  is the void ratio function proposed by Hardin and Richart (1963) for sand with round particles.

Cubrinovski and Ishihara (1998a) suggested that there exists a linear correlation between  $(\tau / p')_{\max}$  and the state index  $I_s$  (Ishihara, 1993), which was used to express the influence of density on stress ratio. Alternatively, in this study, the following linear correlation between  $(\tau / p')_{\max}$  and  $e_0$  is derived from undrained torsional shear tests:

$$(\tau / p')_{\max} = r_1 + r_2 e_0 \quad (19)$$

where  $r_1$  and  $r_2$  are the intercept and the gradient, respectively, in the plot  $(\tau / p')_{\max}$  vs.  $e_0$ .

#### 4.2 Elastic shear strain

In the model, the elastic shear strain increment ( $d\gamma^e$ ) is calculated as formulated in the quasi-elastic constitutive model proposed by HongNam and Koseki (2005):

$$d\gamma^e = d\tau / G \quad (20)$$

$$G = G_{\text{ic}} \frac{f(e)}{f(e_{\text{ic}})} \left( \frac{\sqrt{\sigma_z' \sigma_r'}}{\sigma_{\text{ic}}'} \right)^n \quad (21)$$

where  $G$  is the current shear modulus;  $f(e)$  is the current void ratio function as defined in Eqn. (18);  $f(e_{\text{ic}})$  is the void ratio function at a reference isotropic confining stress  $\sigma_{\text{ic}}'$ ;  $G_{\text{ic}}$  is the initial shear modulus at  $e_{\text{ic}}$  and  $\sigma_{\text{ic}}'$ , as defined in Eqn. (17);  $\sigma_z'$  and  $\sigma_r'$  are the vertical and radial effective stress, respectively; and  $n$  is the same material parameter used in Eqn. (17).

In the proposed model neither  $\sigma_z'$  nor  $\sigma_r'$  are defined as variables. Thus, for simplicity and with negligible errors, Eqn. (21) is replaced by Eqn. (22), which can be derived from Eqn. (17) considering  $G_n = [G/(p')^n]/f(e)$ :

$$G = G_{\text{ic}} \frac{f(e)}{f(e_{\text{ic}})} \left( \frac{p'}{p_{\text{ic}}'} \right)^n \quad (22)$$

#### 4.3 Stress-dilatancy characteristics

Volume change in drained shear tests can be considered as the mirror image of pore water pressure build-up during undrained shear tests. Change of volumetric strain in different stages of shear loading can be described by the stress-dilatancy relationship, which relates the dilatancy ratio ( $-d\varepsilon_{\text{vol}}^p/d\gamma^p$ ) to the stress ratio ( $\tau / p'$ ) (e.g. Pradhan et al., 1989 a, b; Shahnazari and Towhata, 2002).

Nevertheless, theoretical stress-dilatancy relations, such as Rowe's equations (Rowe, 1962), are not directly applicable to the case of torsional shear loading. However, the results from torsional shear tests suggest that unique relationships between  $-d\varepsilon_{\text{vol}}^p/d\gamma^p$  and  $\tau / p'$  exist either for loading ( $d\gamma^p > 0$ ) and unloading ( $d\gamma^p < 0$ ) conditions (Pradhan et al., 1989a,b). Nishimura and Towhata (2004) proposed the following empirical linear stress-dilatancy relationship for sands undergoing torsional shear loading:

$$\frac{\tau}{p'} = N_d \left( -\frac{d\varepsilon_{\text{vol}}^p}{d\gamma^p} \right) + C_d \quad (23)$$

where  $N_d$  and  $C_d$  are the gradient and the intercept of linear relationship, respectively, as schematically shown in Figure 3.

It is important to make clear that  $C_d$  represents the stress ratio at the phase transformation  $(\tau / p')_{\text{PTL}}$  or stress ratio at zero dilatancy state:

$$C_d = (\tau / p')_{\text{PTL}} \quad (24)$$

On the other hand,  $N_d$  is a density dependent parameter. In general, the denser the soil, the greater the  $N_d$  i.e. a denser sand behaves more dilative (Figure 3). In the model, to account for the effect of density on stress ratio and volumetric strain behavior of sand, the following formulation for  $N_d$  is proposed:

$$N_d = d_1 + d_2 e_0 \quad (25)$$

where  $d_1$  and  $d_2$  are two parameters to express the dependence of  $N_d$  on density. The coefficients  $d_1$ ,  $d_2$  and  $(\tau/p')_{PTL}$  obtained for Toyoura sand subjected to torsional shearing are presented later.

It is worth mentioning that for  $d\gamma^p > 0$  (i.e. monotonic shear loading) the following concept is applicable:

- sand behaves contractive when  $0 < \tau/p' < (\tau/p')_{PTL}$ ;
- zero dilatancy state at phase transformation, i.e.  $\tau/p' = (\tau/p')_{PTL}$ ;
- sand behaves dilative when  $\tau/p' > (\tau/p')_{PTL}$ .

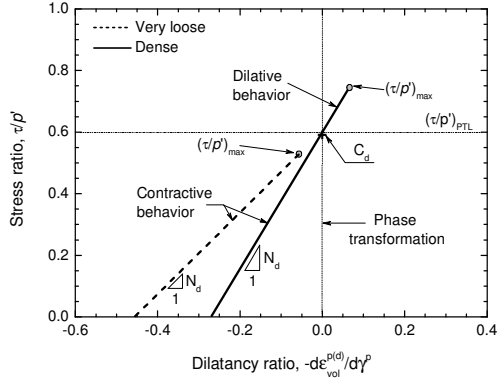


Figure 3 Illustration of stress-dilatancy characteristics for sand subjected to torsional shear

#### 4.4 Excess pore water pressure generation

In modeling the undrained shear behavior, it is assumed that the plastic volumetric strain increment ( $d\varepsilon_{vol}^p$ ) during undrained loading, which consists of dilatancy ( $d\varepsilon_{vol}^{p(d)}$ ) and consolidation/swelling ( $d\varepsilon_{vol}^{p(c)}$ ) components, is equal to zero. In fact, a change of effective mean stress ( $p'$ ) during undrained loading causes re-compression/swelling of the specimen. On the other hand, a change of shear stress ( $\tau$ ) causes the dilatation of the specimen. Therefore, the following equation is valid during undrained loading:

$$d\varepsilon_{vol}^p = d\varepsilon_{vol}^{p(c)} + d\varepsilon_{vol}^{p(d)} = 0 \quad (26)$$

Experimental evidences suggest that the bulk modulus  $K$  ( $= dp'/d\varepsilon_{vol}^{p(c)}$ ) can be expressed as a unique function of  $p'$ :

$$K = \frac{dp'}{d\varepsilon_{vol}^{p(c)}} = K_{ic} \frac{f(e)}{f(e_{ic})} \left( \frac{p'}{p_{ic}'} \right)^m \quad (27)$$

where  $K_{ic}$  is the bulk modulus at reference effective mean stress ( $p_{ic}'$ );  $f(e)$  and  $f(e_{ic})$  are the void ratio function at current and reference stress state, respectively; and  $m$  is a coefficient to model the stress-state dependency of  $K$ .

In the case  $f(e_{ic})=f(e_0)$ ,  $p_{ic}'=p_0'$  and  $K_{ic}=K_0$ , considering that  $f(e)=f(e_0)$  in undrained tests, from Eqns. (26) and (27), the change of effective mean stress (or generation of pore water pressure) during undrained shearing is evaluated as follows:

$$dp' = K_0 \left( \frac{p'}{p_0'} \right)^m (-d\varepsilon_{vol}^{p(d)}) \quad (28)$$

where from Eqn. (23):

$$-d\varepsilon_{vol}^{p(d)} = \frac{1}{N_d} \left( \frac{\tau}{p'} - C_d \right) d\gamma^p \quad (29)$$

Similarly to  $G_0$ , also the initial bulk modulus ( $K_0$ ) may be evaluated by an empirical relationship that considers the effects of initial pressure level ( $p_0'$ ) and void ratio ( $e_0$ ):

$$K_0 = K_m \frac{(2.17 - e_0)^2}{1 + e_0} \left( \frac{p_0'}{p_{ref}'} \right)^m \quad (30)$$

where  $K_m$  is a soil compressibility parameter;  $p_{ref}'$  is a reference stress ( $=100$  kPa) and  $m$  is a soil parameter to express the stress-

level dependence of  $K_0$ . Both  $K_m$  and  $m$  are presented later for the case of Toyoura sand.

## 5. DETERMINATION OF MODEL PARAMETERS

The proposed model requires a unique set of 17 parameters for simulating monotonic undrained torsional shear behavior of saturated sand over a wide range of void ratios and confining pressures. These parameters are related to the GHE ( $C_{1(0)}$ ,  $C_{1(\infty)}$ ,  $\alpha$ ,  $a$ ,  $C_{2(0)}$ ,  $C_{2(\infty)}$ ,  $\beta$ ,  $b$ ), shear modulus ( $G_n$ ,  $n$ ), peak stress ratio ( $r_1$ ,  $r_2$ ), dilatancy ( $d_1$ ,  $d_2$ ,  $(\tau/p')_{PTL}$ ) and bulk modulus ( $K_m$ ,  $m$ ). The model parameters calibrated for Toyoura sand are summarized in Table 1.

Table 1 Model parameters for Toyoura sand (air pluviation)

Relation	Unit	Soil parameters	
GHE strain-function:	---	$C_{1(0)}$	4.0
$C_{1(x)}$		$C_{1(\infty)}$	0.123
		$\alpha$	0.01073
		$a$	0.2
GHE strain-function:	---	$C_{2(0)}$	0.102
$C_{2(x)}$		$C_{2(\infty)}$	1.2
		$\beta$	0.85012
		$b$	0.2
Shear modulus:	kPa	$G_n$	81969.0
$G_0$		$n$	0.51
Peak stress ratio:	---	$r_1$	1.828
$(\tau/p')_{max}$		$r_2$	-1.406
Stress-dilatancy:	---	$d_1$	5.793
$N_d$ ; $C_d$		$d_2$	-5.0
		$(\tau/p')_{PTL}$	0.6
Bulk modulus:	kPa	$K_m$	47710.0
$K_0$		$m$	0.50

### 5.1 GHE parameters ( $C_{1(0)}$ , $C_{1(\infty)}$ , $\alpha$ , $a$ , $C_{2(0)}$ , $C_{2(\infty)}$ , $\beta$ , $b$ )

Figure 4 shows the determination of the GHE parameters. They are obtained by fitting the results of an undrained torsional shear test conducted on a loose Toyoura sand specimen ( $e_0 = 0.828$ ), which was consolidated at  $p_0' = 100$  kPa. The specimen was prepared by the air pluviation method proposed by De Silva et al. (2006) and its size (referred hereafter as medium size) was 300 mm in height, 150 mm in outer diameter and 90 mm in inner diameter. Refer to Chiaro (2010) and Chiaro et al. (2012) for details of torsional shear apparatus and test procedure employed.

Parameters  $C_{1(0)}$ ,  $C_{1(\infty)}$ ,  $C_{2(0)}$  and  $C_{2(\infty)}$  were evaluated graphically as shown in Figure 4. Alternatively,  $\alpha$  and  $\beta$  were calculated using Eqns. (11) and (12), in which reference parameters  $C_{1(x=1)}$  and  $C_{2(x=1)}$  were used together with the already obtained  $C_{1(0)}$ ,  $C_{1(\infty)}$ ,  $C_{2(0)}$  and  $C_{2(\infty)}$ . Lastly, parameters  $a$  and  $b$  were set by trial and error as shown in Figure 4.

### 5.2 Initial shear modulus parameters ( $G_n$ , $n$ )

As shown in Figure 5, for Toyoura sand  $G_n = 81969$  and  $n = 0.51$  are suitable values to fit results of two series of torsional shear tests by Kiyota et al. (2006) and De Silva (2008). These tests were performed on medium size Toyoura sand specimens of various density by applying small amplitude cyclic torsional shear loading at different stages of isotropic consolidation (from 100 to 400 kPa) and isotropic unloading (from 400 to 100 kPa).

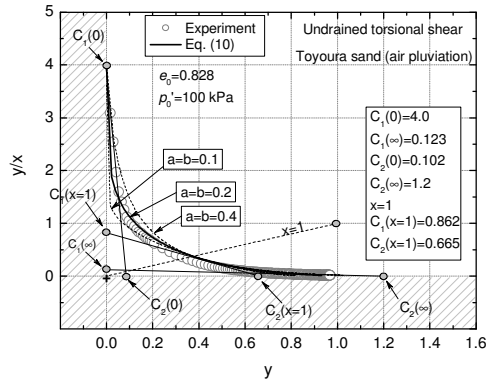


Figure 4 Determination of GHE model parameters for Toyoura sand

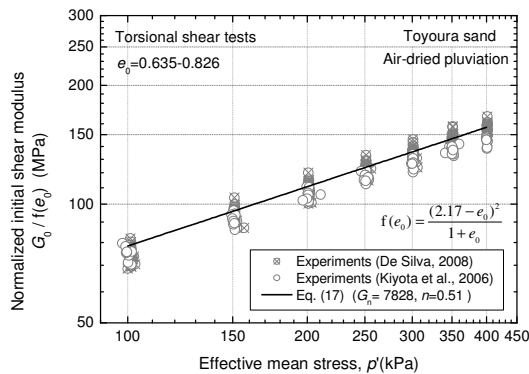


Figure 5 Variation of normalized initial shear modulus with effective mean stress

5.3 Peak shear stress parameters ( $r_1, r_2$ )

Peak stress ratio  $(\tau/p')_{max}$  is a density dependent factor as described by Eqn. (19). Figure 6 shows the correlation between  $(\tau/p')_{max}$  and  $e_0$  obtained from undrained torsional shear tests on medium size Toyoura sand specimens over a wide range of density. Parameters  $r_1 = 1.828$  and  $r_2 = -1.406$  are determined by linearly fitting the experimental data.

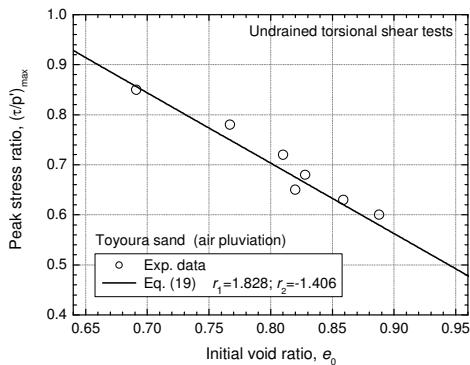


Figure 6 Variation of undrained peak stress ratio with void ratio

5.4 Dilatancy parameters ( $d_1, d_2, (\tau/p')_{PTL}$ )

Simulation results presented in Figure 7 show the value of  $N_d$  obtained by fitting experimental data from undrained torsional shear tests on Toyoura sand. It appears that  $N_d$  decreases with an increase in void ratio i.e.  $N_d$  is greater for denser sand that behaves more dilatant than loose sand. Finally, parameters  $d_1 = 5.793$  and  $d_2 = -5.0$  are obtained by the linear fitting of data presented in Figure 7.

For a given material, the stress ratio at phase transformation  $(\tau/p')_{PTL}$  is independent of void ratio, stress level and drainage conditions (Georgiannou *et al.*, 2008; among others) as well as of initial static shear effects (Chiaro *et al.*, 2012). Thus,  $(\tau/p')_{PTL}$  can be regarded as constant. Based on tests results reported in Chiaro *et al.*

(2012) for medium size Toyoura sand specimens subjected to undrained torsional shear, it is obtained that  $(\tau/p')_{PTL} = 0.6$ .

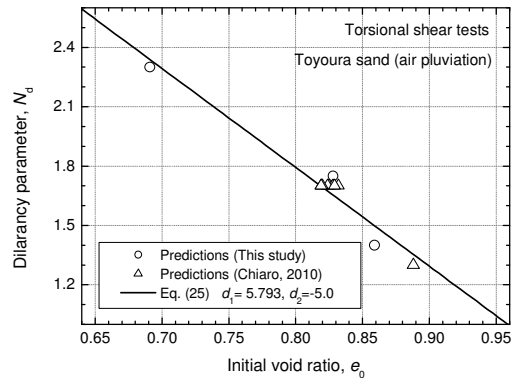


Figure 7 Variation of dilatancy parameter  $N_d$  with void ratio

5.5 Initial bulk modulus parameters ( $K_m, m$ )

Parameters  $K_m$  and  $m$  are taken as 47710 and 0.50, respectively, as proposed in Chiaro (2010) for the case of medium size Toyoura sand specimens subjected to isotropic unloading.

6. MODEL PERFORMANCE

The model is used here to predict the undrained torsional shear behavior of Toyoura sand and compare it with the laboratory observed response. Model predictions cover isotropically and anisotropically (i.e. two-stage drained to undrained shear, as will be described in details in 6.4) consolidated sands. All predictions are obtained using the single set of model parameters listed in Table 1.

6.1 Undrained behavior of sand isotropically consolidated at different density states

Figure 8 compares the predicted and observed behavior of three Toyoura sand specimens consolidated to  $e_0$  of 0.859 (loose), 0.820 (medium dense) and 0.691 (dense) at a confining pressure of 100 kPa. Loose sand shows a predominant contractive behavior with strain-softening, while dense sand behaves predominantly dilatant with strain-hardening.

Despite the change in density with associate contractive/dilatant behavior, the undrained response of sand can be satisfactorily captured by the proposed model in terms of stress-strain relationship, effective stress path and excess pore water pressure characteristics.

6.2 Undrained behavior of sand isotropically consolidated at different stress levels

A tendency for decreasing dilatancy at higher stress levels is a common characteristic of sands as shown by Verdugo and Ishihara (1996), who conducted a series of undrained triaxial compression tests on Toyoura sand specimens consolidated at stress levels increasing from 100 kPa to 3000 kPa.

As far as the authors have investigated the literature, undrained behavior of sand in torsional shear tests has been reported only for confining pressure up to 300 kPa (e.g. Georgiannou and Tsomokos, 2008), which yet well represents the stress levels of interests for many practical geotechnical problems. These tests revealed that for the range of confining pressure investigated, sand behavior does not change toward a more contractive behavior, but rather it remains unaffected.

In Figure 9, behavior of medium dense Toyoura sand is predicted taking into consideration the same confining pressure ( $p_0' = 75, 130, 215$  and  $300$  kPa) employed by Georgiannou and Tsomokos (2008). Similarly to experimental evidences, it can be seen that predicted sand behavior appears to remain unaffected by the confining pressure level. As shown in Figure 9a, independently of stress level, the stress state increases up to a transient peak

(identified by the instability line, IL), then decreases until the phase transformation line (PTL) and, finally, it follows the failure envelope.

Yet, authors admit that possible effects of the confining pressure on the dilatancy characteristics (such as those reported by Verdugo and Ishihara, 1996) may be not fully taken into account in the proposed model, due to insufficient number of relevant experimental data that can be employed for improving the present modelling.

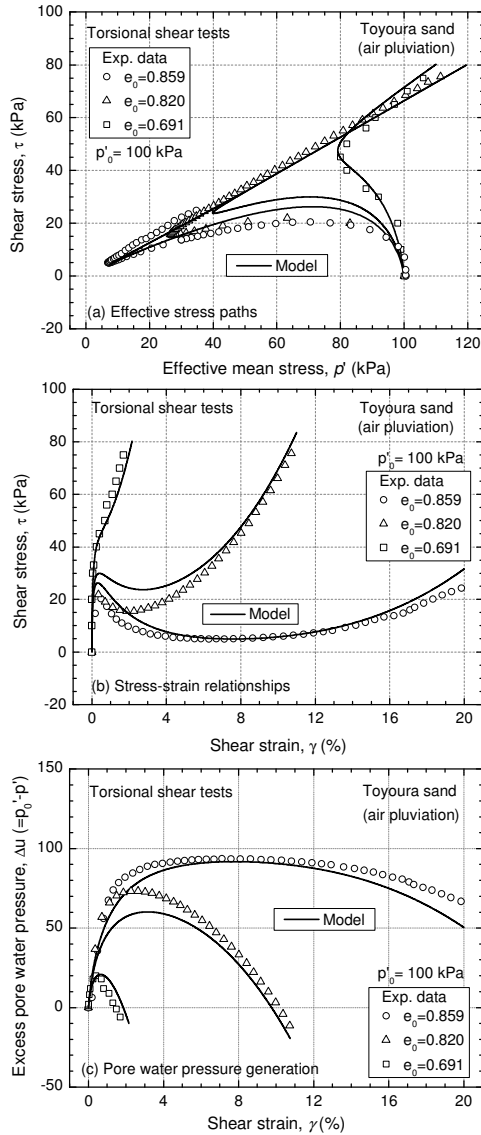


Figure 8 Comparison between experimental and predicted undrained monotonic behavior of Toyoura sand

### 6.3 Static liquefaction behavior of very loose sand

Ishihara (1993) noted that Toyoura sand consolidated to void ratios higher than 0.930 (i.e. very loose state) completely liquefies and exhibits zero residual shear strength under monotonic undrained triaxial compression loading. Later, Yoshimine and Ishihara (1998) reported similar behavior also for very loose Toyoura sand subjected to torsional shear loading.

Figure 10 shows model predictions for undrained torsional shear behavior of Toyoura sand consolidated to  $e_0 = 0.902$  ( $D_r = 25\%$ ) and confining pressure ranging from 50 kPa to 400 kPa. Despite the increase in confining pressure, very loose sand always reaches the full liquefaction state. However, the higher the confining pressure, the greater the shear stress level required to exceed the transient undrained soil strength and consequently trigger liquefaction under monotonic shearing conditions.

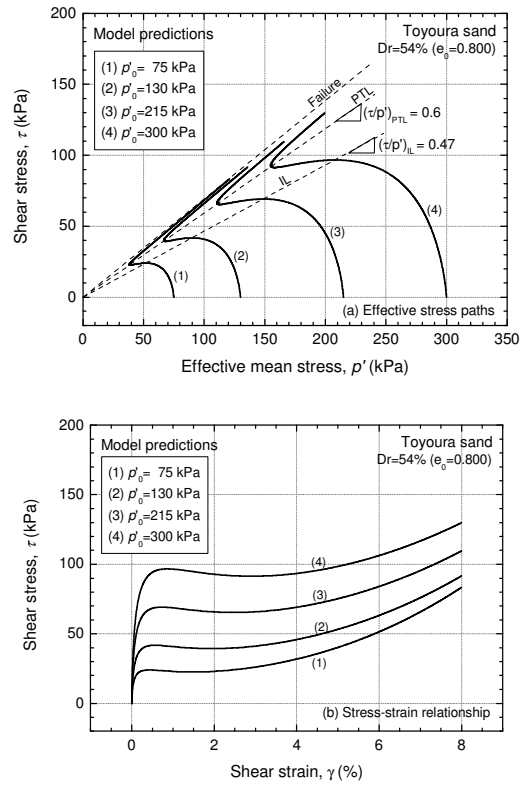


Figure 9 Model predictions of undrained behavior for medium dense Toyoura sand consolidated at different confining pressures

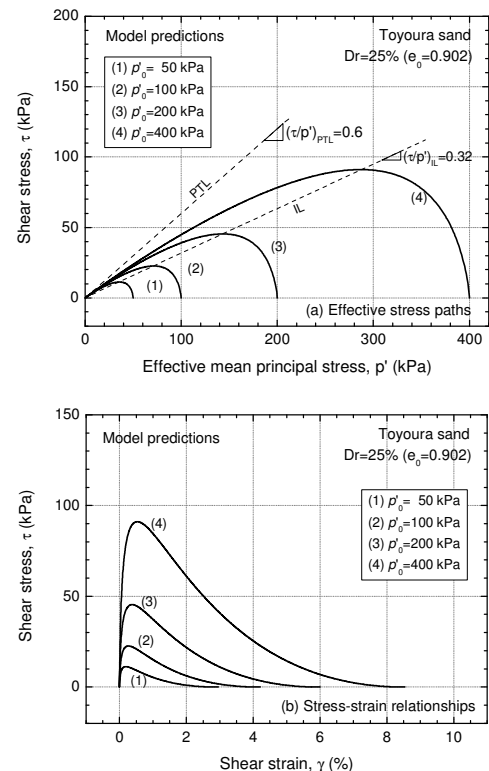


Figure 10 Model predictions of static liquefaction behavior for very loose Toyoura sand consolidated at different confining pressures

### 6.4 Two-stage drained to undrained tests

Two-stage drained to undrained tests are often performed to evaluate the effects of initial static shear (i.e. sloped ground conditions) on the undrained behavior of sand. In the case of torsional shear tests, to apply an initial static shear stress,

isotropically consolidated specimens are subjected to drained torsional shear loading before undrained shearing.

Figure 11 shows model predictions for the test results presented by Arangelowski and Towhata (2004) on Toyoura sand specimens consolidated to  $e_0 = 0.820$ , confining pressure of 196 kPa and sheared under drained, fully undrained (i.e. with zero shear stress) and undrained conditions with static shear of 30, 60 and 90 kPa.

Arangelowski and Towhata (2004) reported that after the shear stress was achieved under drained conditions and undrained loading was applied, an increase in the shear stress was observed and then softening started. However, one exception was the case when initial static shear was rather higher ( $\tau_{static} = 90$  kPa) where instantaneous softening occurred.

According to Lade and Yamamuro (2011), initiation of instability (i.e. sudden softening) requires that stress state be located into the region of potential instability (i.e. above the IL). However, sand will remain perfectly stable inside the failure surface as long as it is drained. A trigger mechanism that cause pore water pressure to increase faster than it can dissipate (i.e. undrained conditions) is required to cause instability.

It is clear that model prediction is well in accordance with experimental data reported in the literature, including a tendency for increasing undrained peak strength of sand due to an increase of initial static shear which has been observed by various researchers (e.g. Hyodo *et al.*, 1994; Vaid *et al.*, 2001; Arangelowski and Towhata, 2004; Chiaro *et al.*, 2012).

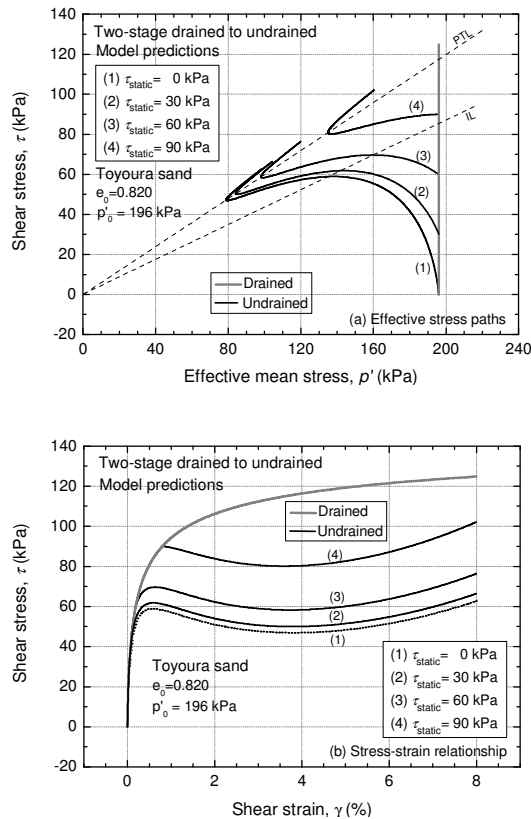


Figure 11 Model prediction for undrained monotonic behavior of Toyoura sand in two-stage drained to undrained tests

## 7. SUMMARY AND CONCLUSIONS

An elasto-plastic model to describe the density- and stress-dependency of saturated sands subjected to monotonic undrained torsional shear loading has been presented in this paper. The model is based on an extended GHE, which is able to simulate the stress-strain soil behavior over a wide range of densities and confining pressure throughout a single set of model parameters. The most important state-dependent stress-dilatancy relationship is established

to account for the effect of density on stress ratio. Such a stress-dilatancy relation is used for modeling the excess pore water pressure generation in undrained shear conditions as the mirror image of volumetric change in drained shear conditions.

By comparing the simulation results with the experimental results, it is shown that the model is able to predict the contractive and dilative behavior of Toyoura sand under loose and dense states, respectively. It can be seen also that strain softening and hardening are well depicted by the simulations.

Moreover, contractive-dilative behavior of medium dense Toyoura sand as well as the static liquefaction behavior with zero residual shear strength of very loose Toyoura sand can be both simulated over a wide range of confining pressures. In addition, the model can be used to evaluate the effects of initial static shear (i.e. shear stress induced by drained shear before the undrained one) on the undrained torsional shear behavior of sand.

## 8. ACKNOWLEDGMENTS

The authors express their sincere gratitude to A/Prof. Takashi Kiyota at the University of Tokyo for providing useful experimental data, and Mr. Takeshi Sato for his invaluable support in the laboratory testing.

## 9. LIST OF SYMBOLS

The following symbols are used in this paper:

- $a$ : GHE parameter
- $b$ : GHE parameter
- $C_d$ : intercept of stress-dilatancy relation
- $C_{1(0)}$ : GHE parameter
- $C_{1(\infty)}$ : GHE parameter
- $C_{1(x)}$ : strain-dependent GHE fitting parameter
- $C_{2(0)}$ : GHE parameter
- $C_{2(\infty)}$ : GHE parameter
- $C_{2(x)}$ : strain-dependent GHE fitting parameter
- $dp'$ : effective mean stress increment
- $d\gamma$ : shear strain increment
- $d\gamma^e$ : elastic shear strain increment
- $d\gamma^p$ : plastic shear strain increment
- $d\epsilon_{vol}^{p(c)}$ : plastic vol. strain increment due to consolidation/swelling
- $d\epsilon_{vol}^{p(d)}$ : plastic volumetric strain increment due to dilatancy
- $d\epsilon_{vol}^p$ : plastic volumetric strain increment
- $d\tau$ : shear stress increment
- $d_1$ : dilatancy parameter
- $d_2$ : dilatancy parameter
- $D_r$ : relative density
- $e$ : current void ratio
- $e_{ic}$ : void ratio at reference isotropic confining stress
- $e_0$ : initial void ratio (i.e. at the end of consolidation)
- $f(e)$ : current void ratio function
- $f(e_{ic})$ : void ratio function at reference isotropic confining stress
- $f(e_0)$ : initial void ratio function
- $F_z$ : vertical axial load
- $G$ : current shear modulus
- $G_{ic}$ : shear modulus at reference isotropic confining stress
- $G_n$ : small strain shear stiffness parameter
- $G_0$ : initial shear modulus
- $H$ : specimen height
- $K$ : current bulk modulus
- $K_{ic}$ : bulk modulus at reference isotropic confining stress
- $K_m$ : compressibility parameter
- $K_0$ : initial bulk modulus
- $m$ : soil parameter for bulk modulus
- $n$ : soil parameter for shear modulus
- $N_d$ : gradient of stress-dilatancy relation
- $p'$ : mean stress
- $p'$ : current effective mean stress or confining stress
- $p_i$ : inner cell pressure
- $p_{ic}'$ : reference confining stress

$p_0$ : outer cell pressure  
 $p_{ref}$ : reference confining stress (= 100 kPa)  
 $p_0'$ : initial effective mean stress or confining stress  
 $r_i$ : inner radius of specimen  
 $r_o$ : outer radius of specimen  
 $r_1$ : peak stress ratio parameter  
 $r_2$ : peak stress ratio parameter  
 $T$ : torque load  
 $x$ : normalized plastic shear strain  
 $y$ : normalized stress ratio  
 $\alpha$ : GHE parameter  
 $\beta$ : GHE parameter  
 $\Delta u$ : excess pore water pressure  
 $\gamma$  (=  $\gamma_{z\theta}$ ): torsional shear strain  
 $\gamma^p$ : plastic shear strain  
 $\gamma_{ref}$ : reference shear strain  
 $\theta$ : circumferential angular displacement  
 $\pi$ : constant (= 3.1415926535)  
 $\sigma_r$ : radial stress  
 $\sigma_z$ : vertical stress  
 $\sigma_\theta$ : circumferential stress  
 $\sigma_1$ : major main stress  
 $\sigma_2$ : intermediate main stress  
 $\sigma_3$ : minor main stress  
 $\sigma_{ic}'$ : reference isotropic confining stress  
 $\sigma_r'$ : effective radial stress  
 $\sigma_z'$ : effective vertical stress  
 $\tau$  (=  $\tau_{z\theta}$ ): torsional shear stress  
 $\tau_{static}$ : initial static shear stress  
 $(\tau/p')_{max}$ : peak stress ratio  
 $(\tau/p')_{PTL}$ : stress ratio at phase transformation

## 9. REFERENCES

- Arangelovski, G. and Towhata, I. (2004): "Accumulated deformation of sand with initial shear stress and effective stress state lying near failure conditions", *Soils and Foundations*, 44(6): 1-16.
- Balakrishnairyer, K. (2000): "Modeling of deformation characteristics of gravel subjected to large cyclic loading", Ph.D. Thesis, Dept. of Civil Eng., University of Tokyo, Japan.
- Chiaro, G. (2010): "Deformation properties of sand with initial static shear in undrained cyclic torsional shear tests and their modeling", Ph.D. Thesis, Dept. of Civil Eng., University of Tokyo, Japan.
- Chiaro, G., De Silva, L.I.N., Kiyota, T. and Koseki, J. (2011): "An elasto-plastic model to describe the undrained cyclic behavior of saturated sand with initial static shear", *Proc. 5<sup>th</sup> International Symposium on Deformation Characteristics of Geomaterials*, Seoul, Korea, Vol. 2: 1026-1033.
- Chiaro, G., Kiyota, T. and Koseki, J. (2013): "Strain localization characteristics of loose saturated Toyoura sand in undrained cyclic torsional shear tests with initial static shear", *Soils and Foundations*, 53(1): in press.
- Chiaro, G., Koseki, J. and Sato, T. (2012): "Effects of initial static shear on liquefaction and large deformation properties of loose saturated Toyoura sand in undrained cyclic torsional shear", *Soils and Foundations*, 52(3): 498-510.
- Cubrinovski, M. and Ishihara, K. (1998 a): "Modelling of sand behaviour based on state concept", *Soils and Foundations*, 38(3): 115-127.
- Cubrinovski, M. and Ishihara, K. (1998 b): "State concept and modified elastoplasticity for sand modelling", *Soils and Foundations*, 38(4): 213-225.
- De Silva, L.I.N. (2008): "Deformation characteristics of sand subjected to cyclic drained and undrained torsional shear loadings and their modeling", Ph.D. Thesis, Dept. of Civil Eng., University of Tokyo, Japan.
- De Silva, L.I.N., Koseki, J., Chiaro, G. and Sato, T. (2012): "A cyclic elasto-plastic model to describe liquefaction behavior of saturated sand", *Soils and Foundations* (submitted for review and possible publication).
- De Silva, L.I.N., Koseki, J. and Sato, T. (2006): "Effects of different pluviation techniques on deformation property of hollow cylinder sand specimens" *Proc. of the International Symposium of Geomechanics and Geotechnics of Particle Media*, Ube, Japan, 29-33.
- Duncan, J.M. and Chang, C.Y. (1970): "Nonlinear analysis of stress and strain of soils", *Journal of Soil Mechanics and Foundation Division, ASCE*, 96(SM5): 1629-1653.
- Georgiannou, V.N. and Tsomokos, A. (2008): "Comparison of two fine sands under torsional loading", *Canadian Geotechnical Journal*, 45(12): 1659-1672.
- Georgiannou, V.N., Tsomokos, A. and Stavrou, K. (2008): "Monotonic and cyclic behaviour of sand under torsional loading", *Geotechnique*, 58(2): 113-124.
- Hardin, B.O. and Drnevich, V.P. (1972): "Shear modulus and damping in soils: design equations and curves", *Journal of Soil Mechanics and Foundation Division, ASCE*, 98(SM7): 667-692.
- Hardin, B. O. and Richart, F. E. (1963): "Elastic wave velocities in granular soils", *Journal of Soil Mechanics and Foundation Division, ASCE*, 89(SM1): 33-65.
- Hight, D.W., Gens, A. and Symes, M.J. (1983): "The development of a new hollow cylinder apparatus for investigating the effects of principal stress rotation in soils", *Feotechnics*, 33(4), 355-383.
- HongNam (2004): "Locally measured quasi-elastic properties of Toyoura sand in cyclic triaxial and torsional loadings", Ph.D. Thesis, Dept. of Civil Eng., University of Tokyo, Japan.
- HongNam, N. and Koseki, J. (2005): "Quasi-elastic deformation properties of Toyoura sand in cyclic triaxial and torsional loadings", *Soils and Foundations*, 45(5): 19-38.
- Hyodo, M., Tanimizu, H., Yasufuku, N. And Murata, H. (1994): "Undrained cyclic and monotonic triaxial behavior of saturated loose sand", *Soils and Foundations*, 34(1): 19-32.
- Imam, S.M.R., Morgenstern, N.R., Robertson, P.K. and Chan, D.H. (2005): "A critical-state constitutive model for liquefiable sand", *Canadian Geotechnical Journal*, 42(6): 830-855.
- Ishihara, K. (1993): "Liquefaction and flow failure during earthquakes", 33<sup>rd</sup> Rankine Lecture, *Geotechnique*, 43(3): 351-415.
- Ishihara, K., Tatsuoka, F. and Yasuda, S. (1975): "Undrained deformation and liquefaction of sand under cyclic stresses", *Soils and Foundations*, 15(1): 29-44.
- Iwasaki, T. and Tatsuoka, F. (1977): "Effects of grain size and grading on dynamic shear moduli of sands", *Soils and Foundations*, 17(3): 19-35.
- Iwasaki, T., Tatsuoka, F. and Takagi, Y. (1978): "Shear modulus of sand under cyclic torsional shear loading", *Soils and Foundations*, 18(1): 39-56.
- Jefferies, M.G. (1993): "Nor-sand: a simple critical state model for sand", *Geotechnique*, 43(1): 91-103.
- Kiyota, T., De Silva, L.I.N., Sato, T. and Koseki, J. (2006): "Small strain deformation characteristics of granular materials in torsional shear and triaxial tests with local deformation measurements", *Geotechnical Symposium in Rome, Soil stress-strain behavior: measurement, modeling and analysis*, Ling et al. (eds.), Rome, Italy, 557-566.
- Kiyota, T., Sato, T., Koseki, J., Mohammad, A. (2008): "Behavior of liquefied sands under extremely large strain levels in cyclic torsional shear tests", *Soils and Foundations*, 48(5): 727-739.
- Kondner, R.B. (1963): "Hyperbolic stress-strain response: cohesive soils", *Journal of Soil Mechanics and Foundation Division, ASCE*, 89(SM1), 115-143.
- Lade, P.V. (1993): "Initiation of static instability in the submarine Nerlerk berm", *Canadian Geotechnical Journal*, 30(6): 895-904.

- Lade, P.V. and Yamamuro, J.A. (2011): "Evaluation of static liquefaction potential of silty sand slopes", *Canadian Geotechnical Journal*, 48(2): 247-264.
- Li, X.S. and Dafalias, Y.F. (2012): "Anisotropic critical state theory: role of fabric", *Journal of Engineering Mechanics, ASCE*, 138(3): 263-275.
- Ling, H.I. and Liu, H. (2003): "Pressure-level dependency and densification behavior of sand through a generalized plasticity model", *Journal of Engineering Mechanics, ASCE*, 129(8): 851-860.
- Ling, H.I., and Yang, S. (2006): "Unified sand model based on the critical state and generalized plasticity", *Journal of Engineering Mechanics, ASCE*, 132(12): 1380-1391.
- Modoni, G., Koseki, J. and Anh Dan, L.Q. (2011): "Cyclic stress-strain response of compacted gravel", *Geotechnique*, 61(6):473-485.
- Modoni, G. and Gazzellone, A. (2011): "Experimental observations on the critical state of granular materials", *Proc. 5<sup>th</sup> International Symposium on Deformation Characteristics of Geomaterials*, Seoul, Korea, Vol. 2: 850-857.
- Nishimura, S. and Towhata, I. (2004): "A three-dimensional stress-strain model of sand undergoing cyclic rotation of principal stress axes", *Soils and Foundations*, 44(2): 103-116.
- Pastor, M., Zienkiewicz, O.C. and Chan, A.H.C. (1990): "Generalized plasticity and modeling of soil behavior", *International Journal for Numerical and Analytical Methods in Geomechanics*, 14(3): 151-190.
- Pradhan, T.B.S. and Tatsuoka, F. (1989 a): "On stress-dilatancy equations of sand subjected to cyclic loadings", *Soils and Foundations*, 29(1): 65-81.
- Pradhan, T.B.S., Tatsuoka, F. and Sato, Y. (1989 b): "Experimental stress-dilatancy relations of sand subjected to cyclic loadings", *Soils and Foundations*, 29(1):45-64.
- Rowe, P.W. (1962): "The stress-dilatancy relation for static equilibrium of an assembly of particles in contact", *Proc. Royal Society of London, Series A*, 269: 500-527.
- Shahnazari, H. and Towhata, I. (2002): "Torsion shear tests on cyclic stress-dilatancy relationship of sand, *Soils and Foundations*, 42(1): 105-119.
- Tatsuoka, F., Masuda, T., Siddiquee, M.S.A. and Koseki, J. (2003): "Modeling the stress-strain relations of sand in cyclic plane strain loading", *Journal of Geotechnical and Geoenvironmental Engineering, ASCE*, 129(6): 450-467.
- Tatsuoka, F., Muramatsu, M. and Sasaki, T. (1982): "Cyclic undrained stress-strain behaviour of dense sands by torsional simple shear stress", *Soils and Foundations*, 22(2): 55-70.
- Tatsuoka, F. and Shibuya, S. (1992): "Deformation characteristics of soils and rocks from field and laboratory tests", *Keynote Lecture, Proc. 9<sup>th</sup> Asian Regional Conference SMFE*, Bangkok, Thailand, Vol. 2: 101-170.
- Tatsuoka, F., Siddiquee, M.S.A., Park, C.S., Sakamoto, M. and Abe, F. (1993): "Modelling stress-strain relations of sand", *Soils and Foundations*, 33(2): 60-81.
- Vaid, Y.P., Cung, E.K.F. and Kuerbis, R.H. (1990): "Stress path and steady state", *Canadian Geotechnical Journal*, 27(1): 1-7.
- Vaid, Y.P., Stedman, J.D. and Sivathayalan, S. (2001): "Confining stress and static shear effects in cyclic liquefaction", *Canadian Geotechnical Journal*, 38(3): 580-591.
- Verdugo, R. and Ishihara, K. (1996): "The steady state of sandy soils", *Soils and Foundations*, 36(2): 81-92.
- Yamamuro, J.A. and Lade, P.V. (1998): "Steady-state concept and static liquefaction of silty sand", *Journal of Geotechnical and Geoenvironmental Engineering, ASCE*, 124(9): 868-877.
- Yoshimine, M. and Ishihara, K. (1998): "Flow potential of sand during liquefaction", *Soils and Foundations*, 38(3): 189-198.